NONHYDROSTATIC STRESS EFFECTS ON BORON DIFFUSION IN SI

MICHAEL J. AZIZ
Division of Engineering and Applied Sciences, Harvard University, Cambridge, MA 02138

ABSTRACT

The thermodynamics of diffusion under hydrostatic pressure and nonhydrostatic stress is developed for single crystals free of extended defects and is applied to the case of boron diffusion in silicon. The thermodynamic relationships obtained permit the direct comparison of hydrostatic and biaxial stress experiments and of atomistic calculations under hydrostatic stress. Assuming various values for the anisotropy in the migration strain, a currently unknown parameter, comparison is made between various measurements under hydrostatic pressure and nonhydrostatic stress, and various atomistic calculations of the volumetrics of B and Si diffusion by an interstitial-based mechanism. An independent determination of the anisotropy of the migration strain would permit a parameter-free determination of the predominant diffusion mechanism and would permit the prediction of the ratio of the diffusivity normal to the free surface to the diffusivity parallel to the surface for biaxially strained films. Procedures for measuring and calculating the anisotropy in the migration strain are described.

INTRODUCTION

Because understanding and controlling diffusion related phenomena become increasingly important as semiconductor device dimensions decrease, diffusion in semiconductors has been heavily studied. Despite this emphasis there remains no consensus about the relative concentrations and mobilities of the point defects involved in the diffusion of many substitutional elements in Si[1]. A study of the dependence of the atomic diffusivity, D, on pressure, p, and stress, σ, can provide valuable information to help elucidate the atomistic mechanism(s) of diffusion[2,3]. It can permit conclusions to be drawn about the predominant point defect mechanism independent of the assumptions inherent in the currently used kinetic models. The only necessary assumption is that the experimental time scale is long enough to permit point defect equilibration between the experimental diffusion zone and the nearest free surface.

To understand the various influences of pressure and stress on the diffusivity[3] we consider separately the effects on the point defect concentrations[3-5] and on the point defect mobilities[6,7].

POINT DEFECT THERMODYNAMICS UNDER STRESS

The thermodynamics of point defect formation under hydrostatic or nonhydrostatic stress in heavily dislocated crystals has been well understood for decades. When experimental conditions are such that the point defect concentrations equilibrate rapidly with the point defect sources and sinks compared to the experimental time scale then the pressure-dependence of the point defect concentration is characterized by the (scalar) formation volume:

$$-kT \frac{\partial \ln C^e(T,p)}{\partial p} \equiv V^f . \qquad (1)$$

The new situation that gives the point defect formation volume in a cubic crystal a tensor character is that large single crystals entirely free of extended defects at which point defects can internally equilibrate are now commonplace. To understand the consequences of this lack of inexhaustible internal sources and sinks for point defects, let us consider the example of vacancy formation in a material where we assume for simplicity that (i) there is a negligible concentration of interstitials in equilibrium; (ii) the equilibrium lattice parameter is independent of temperature; (iii) the elastic

moduli are infinite; and (iv) there is no relaxation of the neighboring atoms inward or outward around the vacancy. All of these simplifying assumptions can be lifted without changing the conclusions qualitatively. Let us first discuss the relevant effects for a bulk single crystal and then discuss the case of a dislocation-free coherently strained epitaxial single crystal thin film.

Bulk Crystals

Start with a perfect, vacancy-free single crystal (cubic lattice) at absolute zero. Say it's 10 cm long in the [100] and [010] directions and 10 μm thick in the [001] direction, as shown in Fig. 1. The (001) and (00 -1) surfaces, which are square, will be referred to as the "broad" surfaces and the other four surfaces as the "lateral" surfaces. Also assume that there is no dislocation injection under nonhydrostatic stress (a situation that can be realized in bulk crystals at sufficiently low stress levels, and in thin films at quite high stress levels). Suddenly heat this "wafer" up to a high temperature, at which the equilibrium vacancy concentration is 10% (one vacant site per ten sites).

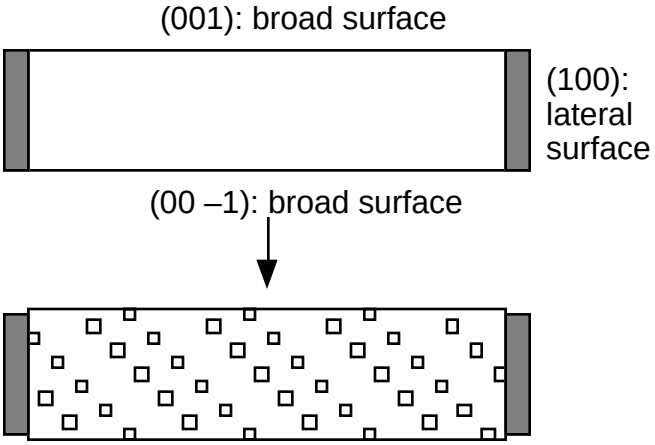

Fig. 1. Top: wafer at low temperature; no point defects. Bottom: wafer raised to high temperature; many vacancies injected. Wafer thickens only in [001] direction if vacancies are injected from broad surfaces. Coating prevents injection from lateral surfaces.

(a) Suppose you coat the lateral surfaces with some material that prevents these surfaces from acting as sources or sinks for point defects, as shown in Fig. 1. In this case vacancies form at the (001) and (00 -1) surfaces (by atoms jumping from their sites in extremal terraces into "adatom" positions, etc.) and diffuse inward. The vacancy concentration in the bulk of the wafer will have equilibrated after a time t_1 given by $z \sim \sqrt{D\, t_1}$, where D is the vacancy diffusivity and z is the wafer thickness (10 μm). As illustrated in Fig. 1, after equilibration the wafer thickness will have increased by 10% (i.e., 1 μm) *but its lateral dimensions will remain completely unchanged*. If instead Frenkel pairs form in the bulk, the self-interstitials will annihilate at the only sinks - the (001) and (00 -1) surfaces, and the final state is exactly the same. If there is a transient internal source of vacancies or interstitials then the transient period will end after the source is exhausted, whereupon the vacancy concentration will attain the same equilibrium value of 10% and the wafer's final width will remain unchanged.

(b) Suppose you now coat the broad (001) and (00 -1) surfaces with this material but strip it off the four lateral surfaces. Upon heating in this case, vacancies form at the lateral surfaces and diffuse inward. The vacancy concentration in the bulk of the wafer will have equilibrated after a much, much longer time t_2 given by $x \sim \sqrt{D\, t_2}$, where x is the wafer length (10 cm). After equilibration the wafer length will have increased by roughly 5% (i.e., 0.5 cm) in each of the two lateral directions, but its thickness will remain completely unchanged.

(c) Now, remove all coatings so that the vacancies can equilibrate at all surfaces. Upon heating, vacancies begin to diffuse in from all surfaces, resulting in the expansion of the crystal in all directions. After a time t_1 the vacancies will have diffused in about 10 μm in all directions, resulting in an expansion of about 1 μm in each of the three dimensions of the crystal, *and equilibration will have occurred*. The final shape will be almost indistinguishable from that in (a).

Now consider the stress-strain work done by the wafer on some agent of compressive stress applied to each set of faces in turn. A gravity-driven device for applying different stresses to each set of faces is shown in Fig. 2. Suppose that, when applying compressive stress to the lateral faces, we can do this without buckling the wafer (alternatively, we could use tensile stress). The coating has been stripped off of all faces. Assume that there are enough steps on the crystal surfaces that vacancies can be formed without changing the surface area. The fraction of vacant lattice sites in equilibrium (neglecting local entropy effects for the sake of simplicity) is a Boltzmann factor in the vacancy formation-induced change in the total energy of the system (energy of the crystal plus gravitational potential energy of the weights). An equivalent alternative statement is that the fraction of vacant lattice sites in equilibrium is a Boltzmann factor in the total energy change of the crystal plus the work done against the agents imposing the stresses.

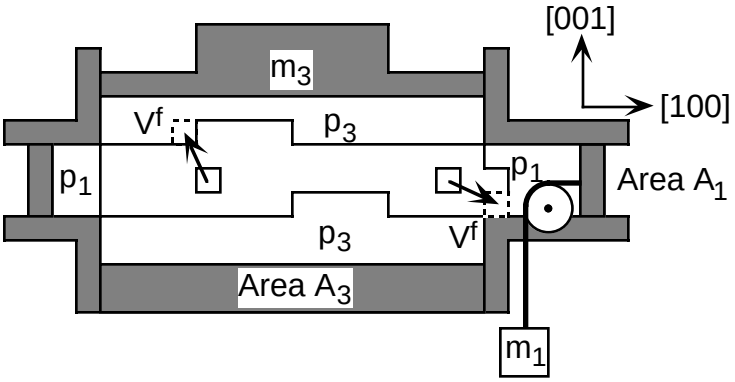

Fig. 2. Work done upon vacancy formation in crystal (middle) with stepped surfaces free of extended defects. Pressures, p_1 and p_3, of incompressible fluids in contact with (100) and (001) faces, respectively, maintained by pistons driven by masses m_1 and m_3. Crystal volume changes by V^f upon vacancy formation at (100) or (001) surface but work done against gravity differs.

(d) If no stress is applied to the broad faces ($m_3 = 0$) but compressive stress $p_1 = m_1 g/A_1$ is applied to all lateral faces at absolute zero and then the wafer heated up to the same temperature as before, every time a vacancy is formed at the broad, free faces no work is done against the source of the stress and so the vacancy formation/annihilation balance at the broad, free faces is unaltered. Vacancy formation at the lateral faces under compressive stress is retarded, because each time a vacancy is formed at the lateral faces the crystal must do work ($p_1 V^f$ in the example shown in Fig. 2) against the agent applying the compressive stress. After a time t_1 vacancy formation/migration near the lateral faces is affected by the presence of the nearby free surfaces and there is a net vacancy transport from the nearby parts of the free surfaces to the lateral surfaces, with a net annihilation at the lateral surfaces (Nabarro-Herring creep). At about t_1 the state is identical to that in (a) except for these edge effects.

(e) If instead we leave the lateral surfaces free and apply compressive stress $p_3 = m_3 g/A_3$ to the (001) and (00 -1) faces then the rate of vacancy creation on these broad surfaces will be reduced but the rate of vacancy creation/annihilation at the lateral surfaces will be identical with the totally unstressed case (c). After a time t_1 the vacancy concentration in the bulk of the wafer will have "equilibrated" at a lower value than 10% because of the work done against the source of the stress. The exception is the material within about 10 μm of the lateral faces, which will have equilibrated with the lateral faces at the stress-free equilibrium value of 10%. During a much, much longer time t_2 the shape will evolve toward that in (b) due to Nabarro-Herring creep. However, the equilibrium vacancy concentration will still be less than 10% because even though vacancies have had time to diffuse in all the way from the wafer edges, they annihilate at the broad surfaces with a much faster time constant, t_1. Consequently, the equilibrium vacancy concentration in the bulk of the wafer remains at the value dictated by the normal stress applied to the nearest surface.

(f) Next, consider a cube of edge length $z_3 = 10$ cm cut from a boule of silicon, with no point defects and no extended defects. Suppose that in an idealized diffusion experiment we deposit a monolayer of radioisotope ^{31}Si on the (001) surface and, after annealing, examine the concentration-depth profile normal to that surface over a depth scale z_4 of nanometers to

millimeters. The depth profile, of course, would be measured far from the edges of the face. At absolute zero, apply "lateral" compressive stress to the (100) & (-1 00) and the (010) & (0 -1 0) faces; then heat up. After a relatively short time given by $z_4 \sim \sqrt{D\, t_4}$, the (001) face will have acted as a source of vacancies, equilibrating the near-surface region in which the experiment is being performed. The work done against the source of lateral compressive stress in forming these vacancies is zero. Hence the lateral compressive stress has no sensible effect on the vacancy concentration in this experiment. After a much longer time given by $z_3 \sim \sqrt{D\, t_3}$, "edge effects" from the lateral faces will start to affect the vacancy concentration in region probed experimentally and only then can the stresses applied to the lateral faces come into play.

Thin Films

Consider a thin film of Si (001) coherently strained to be lattice-matched to a strain-relaxed Si-Ge alloy substrate. Let the film thickness be $z_5 \sim 1\ \mu m$. Here we generalize the discussion to pertain to both vacancies and self-interstitials. If the only significant source/sink is the free surface (i.e., there is an insignificant amount of point defect equilibration on threading dislocations), then heating from low temperature will result in point defect injection from the free surface of the film. After a time given by $z_5 \sim \sqrt{D\, t_5}$ the point defect concentration throughout the film will have reached its value in equilibrium with the free surface. In the absence of relaxation around the vacancy or self-interstitial, this will be identical to the value in the unstrained material.

Inclusion of Nonzero Relaxation and Mobility Effects

Now let us permit relaxation of the neighbors of the vacancy or self-interstitial. This relaxation propagates out isotropically to the surfaces of the sample resulting in a volume change V^r (which is positive if the relaxation is outward and negative if the relaxation is inward). Unlike the volume change upon creation of relaxation-free point defects, the volume change upon relaxation interacts with the normal tractions applied to all surfaces. For point defects formed at the (001) surface, the dimension changes of the crystal upon point defect formation can be described by the "formation strain tensor" $\mathbf{V^f}$:

$$\mathbf{V^f} = \pm\Omega \begin{bmatrix} 0 & & \\ & 0 & \\ & & 1 \end{bmatrix} + \frac{V^r}{3} \begin{bmatrix} 1 & & \\ & 1 & \\ & & 1 \end{bmatrix}, \qquad (1)$$

where Ω is the lattice site volume. The + sign is for vacancy formation and the – sign is for interstitial formation throughout this paper. In all the examples discussed above, the dependence of the equilibrium vacancy concentration on applied stress σ can be written

$$\frac{C^e(\sigma)}{C^e(\mathbf{0})} = \exp\left(\frac{\sigma \cdot \mathbf{V^f}}{kT}\right), \qquad (2)$$

where $\mathbf{V^f}$ has the elements 0 and 1 placed appropriately in (1) for the surface at which the defects equilibrate. In general the defect mobility, **M**, in directions parallel and perpendicular to the direction of applied stress differ[6,7]. Typically we measure D_{33}, the diffusivity in a direction normal to the film surface, which depends on M_{33}, the mobility in this direction. The effect of stress on M_{33} is characterized by the migration strain tensor, given by:

$$\mathbf{V^m_{33}} = \begin{bmatrix} V^m_\perp & & \\ & V^m_\perp & \\ & & V^m_\parallel \end{bmatrix}. \qquad (3)$$

$V_{\parallel}^{m}$ and $V_{\perp}^{m}$, respectively, are the dimension changes of the crystal parallel and perpendicular to the direction of net transport when the point defect reaches its saddle point. As the diffusivity is proportional to the product of the concentration and mobility of point defects, the effect of stress on the diffusivity in the direction normal to the film surface is obtained by the combination of (1) and (3):

$$kT \ln \frac{D_{33}(\sigma)}{D_{33}(\mathbf{0})} = \sigma \cdot \mathbf{V_{33}^{*}} ; \tag{4}$$

$$\mathbf{V_{33}^{*}} = \mathbf{V^{f}} + \mathbf{V_{33}^{m}}. \tag{5}$$

Hydrostatic pressure then influences D_{33} according to

$$\frac{D_{33}(p)}{D_{33}(0)} = \exp\left(\frac{-p[\pm\Omega + V^{r} + V^{m}]}{kT}\right), \tag{6}$$

where the conventionally-defined scalar activation volume V* is the sum of the bracketed terms in (6) and the conventionally-defined scalar migration volume V^{m} is the trace of (3). Biaxial stress influences D_{33} according to

$$\frac{D_{33}(\sigma_{biax})}{D_{33}(0)} = \exp\left(\frac{\sigma_{biax}\left[\frac{2}{3}V^{r} + V^{m} - V_{\parallel}^{m}\right]}{kT}\right). \tag{7}$$

Experimentally, the influence of biaxial stress has been characterized by the apparent change in activation energy with biaxial (tensile) strain, ε, at constant composition:

$$Q' = -kT\frac{\partial \ln D_{33}}{\partial \varepsilon} \tag{8}$$

By comparison to (7), the combination of volumes in square brackets in (7) is equal to –Q'/Y, where the biaxial modulus Y is the ratio of Young's modulus to one minus Poisson's ratio.

For any point defect mechanism, the three parameters V^{r}, $V_{\parallel}^{m}$, and $V_{\perp}^{m}$ can now be calculated using molecular statics or dynamics simulations and the results used to predict the measured behavior through (6) and (7), respectively. However, in principle it is possible to measure these parameters independently. Hydrostatic and biaxial stress experiments, through (6) and (7), provide two equations in the three variables V^{r}, $V_{\parallel}^{m}$, and $V_{\perp}^{m}$. A third experiment is needed to uniquely identify these parameters from experimental measurements alone. One such experiment would be the effect of biaxial stress upon D_{11}, the diffusivity *in a direction parallel to the film surface*, as shown in Fig. 3. This measurement might be made by examining the strain-dependence of the electrical characteristics of a transistor fabricated on a Si thin film coherently strained on a series of strain-relaxed Si-Ge alloys of different compositions. D_{11} depends on M_{11}, the mobility in the [100] direction. The effect of stress on M_{11} is characterized by a migration strain tensor given by

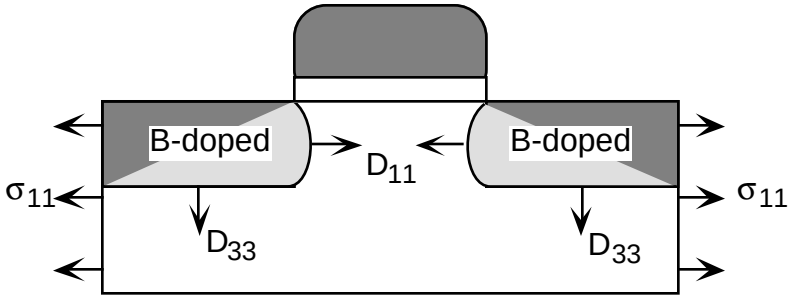

Figure 3. Experiment for determining effect of biaxial stress on diffusion parallel to surface, thereby permitting independent experimental determination of all three parameters V^r, $V_{\parallel}^m$, and $V_{\perp}^m$

$$\mathbf{V_{11}^m} = \begin{bmatrix} V_{\parallel}^m & & \\ & V_{\perp}^m & \\ & & V_{\perp}^m \end{bmatrix}. \tag{9}$$

The effect of stress on the D_{11} is obtained by the combination of (1) and (9):

$$kT \ln \frac{D_{11}(\sigma)}{D_{11}(\mathbf{0})} = \sigma \cdot \mathbf{V_{11}^*}\ ; \tag{10}$$

$$\mathbf{V_{11}^*} = \mathbf{V^f} + \mathbf{V_{11}^m}; \tag{11}$$

$$\frac{D_{11}(\sigma_{biax})}{D_{11}(0)} = \exp\left(\frac{\sigma_{biax}\,[\frac{2}{3}V^r + V^m + V_{\parallel}^m]}{kT}\right). \tag{12}$$

Combining (7) and (12), the anisotropy in the diffusivity itself can be found:

$$\frac{D_{11}(\sigma_{biax})}{D_{33}(\sigma_{biax})} = \exp\left(\frac{\sigma_{biax}\,[V_{\parallel}^m - V_{\perp}^m]}{kT}\right). \tag{13}$$

COMPARISON OF THEORY AND EXPERIMENT

In the absence of atomistic calculations or the D_{11} experiment, let us examine and compare the calculations and experiments that have been performed to date. Combining (3), (6), (7), and (8), we find

$$V^* + \frac{3}{2}\frac{Q'}{Y} = \pm\,\Omega + (V_{\parallel}^m - V_{\perp}^m). \tag{14}$$

In interpreting atomistic calculations and experiments in the past, the assumption has been made almost universally that V^m is negligible. If instead we make the less restrictive assumption that the *anisotropy* in $\mathbf{V^m}$ is negligible, then the right-hand side of (14) should be +1 Ω for a vacancy mechanism and -1 Ω for an interstitial-based mechanism. Let us examine the experiments for boron diffusion in Si assuming an interstitial-based mechanism and observe the effects of various

assumptions about the magnitude of the anisotropy. It seems very unlikely that $(V_{\parallel}^{m} - V_{\perp}^{m})$ could be greater in magnitude than about 1Ω and so we will assume values of $-\Omega/2$, 0, and $+\Omega/2$ in our calculations.

We know of no atomistic calculations of the volumetrics of boron diffusion in silicon. However, relaxation volumes have been calculated for self diffusion by interstitial-based mechanisms. Antonelli and Bernholc[8] used density functional theory with the local density approximation to calculate the volume of formation of the self-interstitial in the tetrahedral and bond-centered configurations. Tang *et al.*[9] used the tight-binding approximation to calculate a formation volume of $-0.1\ \Omega$ for the <110> dumbbell self interstitial. If we assume that the formation and migration volumes for boron diffusion are close to those for self diffusion then we can use these Si results as a proxy for the boron results.

Experimentally, Kuo *et al.*[10] isolated the effects of strain and composition on B diffusion in biaxially strained Si-Ge alloy thin films. Their results are the plotted data points in Fig. 4; the slope within a data series represents the strain effect and the offset between data series represents the composition effect. Also, Cowern *et al.*[11] studied Si-Ge interdiffusion in biaxially strained multilayers under inert and oxidation-enhanced conditions and used a model to isolate the effect of strain on the interstitial-based component. They reported a value of $Q' = -12 \pm 6$ eV per unit strain for the interstitial contribution to oxidation-enhanced diffusion (OED). Finally, Zhao *et al.*[2] reported a preliminary measurement of the activation volume for boron diffusion in Si under hydrostatic pressure.

In Fig. 4 we use Eq. (14) to compare the measured and predicted strain-dependence of boron diffusion perpendicular to the surface in biaxially strained Si-Ge. The assumptions made are as follows. (1) The biaxial strain-effect predictions made from the hydrostatic calculations and experiment are plotted on this figure assuming the anisotropy in the migration strain $V_{\parallel}^{m} - V_{\perp}^{m} = 0$ or $\pm\ \Omega/2$ as indicated. For the results of Kuo *et al.* and Cowern *et al.*, which were obtained on biaxially strained films, no assumption is necessary; note their invariance in the three plots. (2) Relaxation and migration volumes for point defects involving boron are assumed identical to those calculated for pure Si (or Ge in the case of Cowern *et al.*). This assumption is not necessary for the experiment of Zhao *et al.* or Kuo *et al.*, which are the only two results for boron diffusion. (3) $V^{m} = 0$ for the <110> dumbbell of Tang *et al.* (4) The biaxial modulus is $Y = 180.5$ GPa independent of composition and temperature. Only the slopes of the curves are relevant - their arbitrary vertical offsets have been chosen to go through 10^{-16} cm^2/s at zero strain. The slopes of the data of Kuo *et al.* for B diffusion in $Si_{89}Ge_{11}$ and $Si_{79}Ge_{21}$ (From their Fig. 2) fall within the range of the other values whereas the slope of their data for B diffusion in pure Si under tensile strain (From their Fig. 3) is opposite in sign. Qualitatively, the similarity of the slopes in curves (a)-(e) and in the alloy data of Kuo *et al.* indicate a consistency with an interstitial-based mechanism whereas their pure Si data do not follow this consistent pattern. It would be very valuable to have calculations and experiments to determine the missing parameters and permit a rigorous comparison. The missing parameters are the formation or relaxation volumes for B diffusion by the interstitialcy or kick-out mechanism in the ground state and at the saddle point of the migration path, and the anisotropy in the migration strain.

CALCULATING ACTIVATION STRAINS

If one has an atomistic mechanism in mind for any kinetic process, the energy and volume changes for the various elementary steps may be calculated using molecular statics or dynamics and the result compared to measured temperature and pressure-dependencies of the kinetic rate

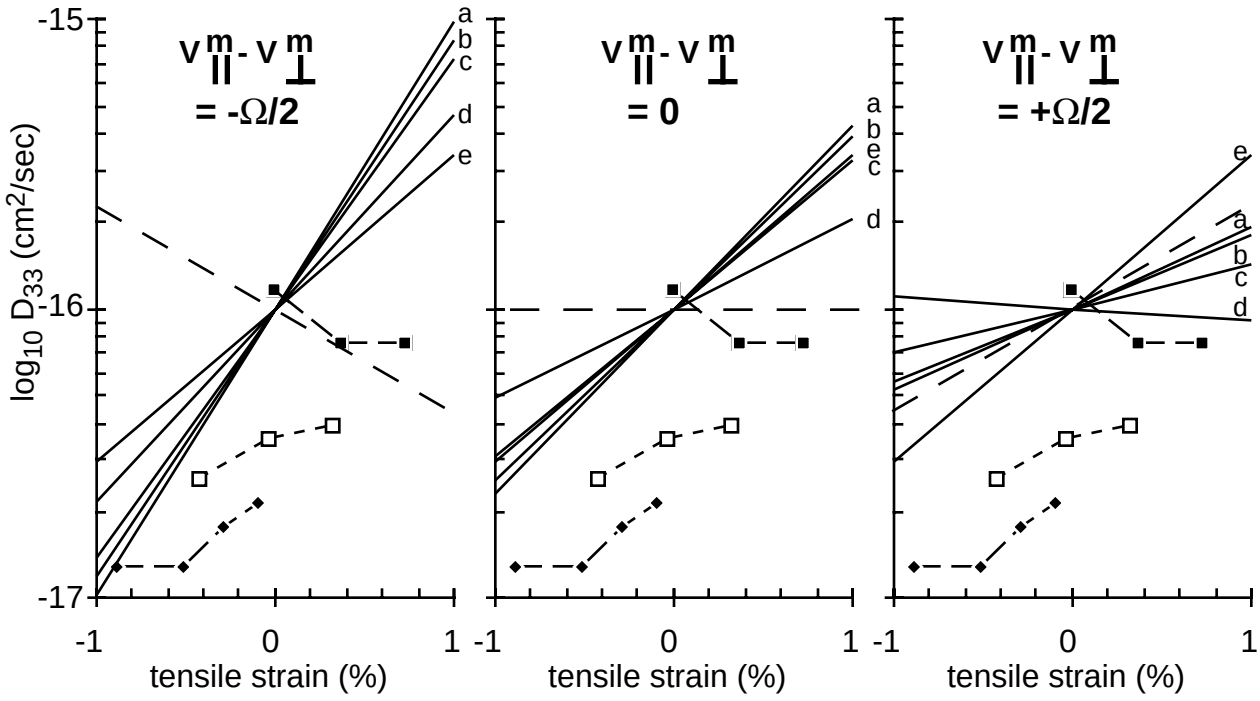

Figure 4. Preliminary comparison of interstitial-based mechanisms in biaxially strained Si-Ge films. Vertical offsets represent composition effect at constant strain; slopes represent strain effect at constant composition. Data from Kuo et al.: filled squares: B in pure Si; open squares: B in $Si_{90}Ge_{10}$; diamonds: B in $Si_{80}Ge_{20}$. Solid lines determined from Eq. (14) using: (a) V^r for <110> dumbbell interstitial in Si self diffusion from Tang et al.; (b) preliminary measurement by Zhao et al. of V for B diffusion in Si; (c) V* for Si self diffusion by tetrahedral interstitial saddle point, from Antonelli and Bernholc; (d) V* for self diffusion by bond-centered interstitial saddle point, from Antonelli and Bernholc; (e) Q' reported for OED of Si/Ge multilayers from Cowern et al. Dashed line: $D_{11}/D_{33} \times 10^{-16}$ cm^2/s, from Eq. (13).*

constant. In general the full tensor character of the volume change (the activation strain) can be calculated and compared with experimental results obtained under nonhydrostatic stress, permitting a more exacting test of the proposed mechanism. In principle the simplest way to calculate the activation strain is identify the nearest-neighboring atoms to the location where the configuration change is occurring and to calculate their displacements out to a distance where nonlinear elastic effects become negligible. Continuum elasticity then permits the evaluation of the displacements of the sample surfaces, which directly gives the activation strain. In practice it has been simplest to calculate the dependence of the energy changes upon the imposed lattice parameter; deducing volume changes in this case requires making assumptions about the entropy changes[8]. A more direct practical method that is now becoming possible is to relax the lattice parameters in a supercell during atomistic configuration changes occurring at zero or constant p or σ; variations in the lattice parameters then give the activation strain tensor directly.

SUMMARY

The thermodynamic relations describing point defect formation and migration in dislocation-free crystals under hydrostatic and nonhydrostatic stress are given by Eqs. (4) and (10).

These relationships permit the direct comparison of hydrostatic and biaxial stress experiments and of atomistic calculations under hydrostatic stress. Assuming various values for the anisotropy in the migration strain the comparison between various measurements under hydrostatic pressure and nonhydrostatic stress, and various atomistic calculations of the volumetrics of B and Si diffusion by an interstitial-based mechanism are qualitatively consistent with an interstitial-based mechanism, with one exception. Procedures for measuring and calculating the anisotropy in the migration strain are described.

This research was supported by NSF-DMR-95-25907. The author is grateful to D.J. Eaglesham and H.-J. Gossmann for much helpful discussion.

REFERENCES

[1]P.M. Fahey, P.B. Griffin and J.D. Plummer, Rev. Mod. Phys. **61**, 289 (1989).

[2]Y. Zhao, M.J. Aziz, S. Mitha and D. Schiferl, Mater. Res. Soc. Symp. Proc. **442**, 305 (1997).

[3]M.J. Aziz, Appl. Phys. Lett. **70**, 2810 (1997).

[4]F.C. Larché and J.W. Cahn, Acta Metall. **33**, 331 (1985).

[5]B.J. Spencer, P.W. Voorhees and S.H. Davis, J. Appl. Phys. **73**, 4955 (1993).

[6]P.H. Dederichs and K. Schroeder, Phys. Rev. B **17**, 2524 (1978).

[7]M.J. Aziz, P.C. Sabin and G.-Q. Lu, Phys. Rev. B **44**, 9812 (1991).

[8]A. Antonelli and J. Bernholc, Phys. Rev. B **40**, 10643 (1989).

[9]M. Tang, L. Colombo, J. Zhu and T. Diaz de la Rubia, Phys. Rev. B **55**, 14279 (1997).

[10]P. Kuo, J.L. Hoyt, J.F. Gibbons, J.E. Turner and D. Lefforge, Appl. Phys. Lett. **66**, 580 (1995).

[11]N.E.B. Cowern, W.J. Kersten, R.C.M. de Kruif, J.G.M. van Berkum, W.B. de Boer, D.J. Gravesteijn and C.W.T. Bulle-Liewma, in Proc. 4th Int. Symp. on Process Physics and Modeling in Semiconductor Devices, eds. G.R. Srinivasan, C.S. Murthy, and S.T. Dunham, Electrochem. Soc. Proc. Vol. 96-4 (Electrochem. Soc., Pennington, NJ, 1996).